JOURNAL OF PROPULSION AND POWER
Vol. 11, No. 6, November–December 1995

Life Prediction of the Thrust Chamber Wall of a Reusable Rocket Engine

Xiaowen Dai* and Asok Ray†
Pennsylvania State University, University Park, Pennsylvania 16802

This article presents a continuous-time structural model of the coolant channel ligament in the thrust chamber wall of a reusable rocket engine such as the Space Shuttle Main Engine. The structural analysis is based on the concepts of sandwich beam approximation and viscoplasticity, and captures the nonlinear effects of creep and plasticity interactions to represent the phenomenological effects of inelastic strain ratcheting, progressive bulging-out, and thinning in the thrust chamber wall. The damage of the thrust chamber wall is quantified as a continuous function of time in terms of the current state of ligament thinning and its critical value. The structural model has been validated for prediction of the ligament thinning by comparison with the finite element models of the thrust chamber wall structure for two different materials, namely, oxygen-free high-conductivity copper and a copper–zirconium–silver alloy called NARloy–Z. The results of parametric studies are presented to show how the service life of the thrust chamber wall is influenced by coolant channel design, ligament material, and load cycle duration. Due to its computational efficiency, this model is suitable for on-line applications of service-life prediction and damage analysis of the thrust chamber wall and also permits parametric studies for off-line synthesis of damage mitigating control systems.

Nomenclature

A	=	cross-sectional area
a_{11}, b_{11}, d_{11}	=	coefficients in stiffness matrix
D	=	damage scaled in the range of 0 to 1
d	=	core thickness of the sandwich beam
d_1, d_2	=	distance between the centroids of the thin faces to the beam midplane in the sandwich beam
E	=	Young's modulus
$\mathcal{L}$	=	predicted value of remaining service life
l	=	half-length of the beam
M	=	bending moment
N	=	tensional force, total number of steps
P	=	pressure
p	=	distributed force per unit length
T	=	absolute temperature
t	=	time
u	=	axial displacement
w	=	radial deflection at the midplane of the beam
x, y, z	=	Cartesian coordinates
α	=	coefficient of thermal expansion
δ_1, δ_2	=	radial deflection of the two faces of the coolant channel ligament
ε	=	strain
η, ξ	=	dummy variable in the integration
ϑ	=	actual thickness of the coolant channel ligament
κ	=	midplane curvature of the coolant channel ligament
σ	=	stress
τ	=	ligament thinning
$\bar{\tau}$	=	normalized ligament thinning
Φ	=	function

Subscripts

B	=	closeout wall
0	=	reference point, reaction load
1	=	coolant side surface of the coolant channel ligament
2	=	hot-gas side surface of the coolant channel ligament

Superscripts

e	=	elastic part
p	=	plastic part
th	=	thermal part
0	=	midplane

Received Nov. 28, 1994; revision received Feb. 17, 1995; accepted for publication Feb. 22, 1995.

*Graduate Student, Mechanical Engineering Department.
†Professor of Mechanical Engineering. Associate Fellow AIAA.

Introduction

FROM the perspectives of engine performance optimization, on-line life prediction, and damage mitigating control,[1–3] the basic requirements for the structural and damage model of reusable rocket engines are numerical efficiency and compatibility with the plant dynamic model. Nonlinear finite element approaches have been reported in literature for analyzing inelastic structures of complex geometry such as the coolant channel ligaments of rocket engines under cyclic loading. Armstrong[4,5] reported inelastic structural analysis of three cylindrical thrust chambers constructed from different copper alloys. Kasper[6] presented structural analysis and life prediction of the coolant channel ligament, made of a copper–zirconium–silver alloy called NARloy–Z, for a typical mission of the Space Shuttle Main Engine. In each of these studies, a structural model based on inelastic nonlinear finite element analysis was used to determine the cumulative plastic deformation leading to thin-out and tensile rupture. However, for on-line life prediction and damage mitigating control, the finite element approach is not practicable because of the exceptionally large requirements of computational resources. An attempt was made by Porowski et al.[7] to formulate a simplified structural model of the coolant channel ligament as a rectangular beam for life prediction of the thrust chamber. Although this approach permits approximate life prediction of the coolant channel ligament at the end of each complete firing cycle, it does not evaluate the intracycle incremental

bulging-out and thinning as continuous functions of time, which is necessary for damage mitigating control.

The previous discussion evinces the need for a new approach to structural and damage modeling of the thrust chamber ligament for on-line life prediction and damage mitigating control. To this effect, this article formulates an analytical model that is built upon the concepts of sandwich beam approximation[8] and viscoplasticity,[9] and captures the nonlinear effects of creep and plasticity interactions to represent the phenomenological effects of inelastic strain ratcheting, progressive bulging-out, and incremental thinning in the thrust chamber wall. The structural and damage models of the coolant channel ligament have been validated by comparison with finite element models, and experimental data for both oxygen-free high-conductivity (OFHC) copper and NARloy–Z. The results of parametric studies are then presented to show how the service life of the chamber wall is influenced by several factors including the ligament material, coolant channel design and configuration, chamber pressure, wall temperature, and loading cycle duration. Due to its computational efficiency, this model is suitable for on-line applications of life prediction and damage mitigating control, and also permits parametric studies for off-line synthesis of damage mitigating control systems.

Structural and Damage Model of the Coolant Channel Wall

The coolant channel ligament, exposed to the hot gases of combustion on one surface and the liquid hydrogen coolant on the other surface as described by Quentmeyer,[10] is shown in Fig. 1. This ligament is represented by an idealized equivalent sandwich beam model,[8] as seen in Fig. 2, where x, y, and z coordinates correspond to the circumferential (hoop), axial, and radial directions of the ligament. For the sandwich beam model to be equivalent to the ligament structure of rectangular cross section in terms of identical deformation in the hoop and radial directions at the midplane, the parameters d_1, d_2, A_1, and A_2 of the sandwich beam, shown in Fig. 2, are chosen such that the cross-sectional area and moment of inertia of the rectangular beam are preserved as

$$d_1 + d_2 = d = (\vartheta/\sqrt{3})$$
$$A_1 = A_2 = (\vartheta/2) \quad \text{for unit length in the } y \text{ direction} \tag{1}$$

where ϑ is the true thickness of the rectangular beam (i.e., the actual coolant channel ligament thickness), d_1 and d_2 are the distances from the centroids of the two faces to the midplane, A_1 and A_2 represent the cross-sectional areas of coolant side and hot-gas side of the ligament for unit length in the y direction, respectively.

The ligament surfaces are also subjected to hydrostatic pressure that exerts distributed force on the wall in the radial z direction. The time-dependent temperature and pressure on the cold side of the ligament are denoted as $T_1(t)$, $P_1(t)$, and on the hot side as $T_2(t)$, $P_2(t)$. The derivation of structural equations that follow is described in detail by Dai and Ray,[11] and the symbols used in these equations are defined in the Nomenclature. Only the pertinent results are summarized in this section. The following general assumptions are made in the development of the governing equations for the structural model:

1) The curvature of the ligament of a single coolant channel is neglected in the undeformed condition due to a large number of such channels.

2) Deformations due to shear are neglected based on the small deflection theory.

3) The sandwich beam model consists of two thin faces with identical thickness θ, which are separated by an incompressible core of thickness $d_1 + d_2 - 2\theta$. Consequently, the local bending stiffness of each thin face is neglected, the normal

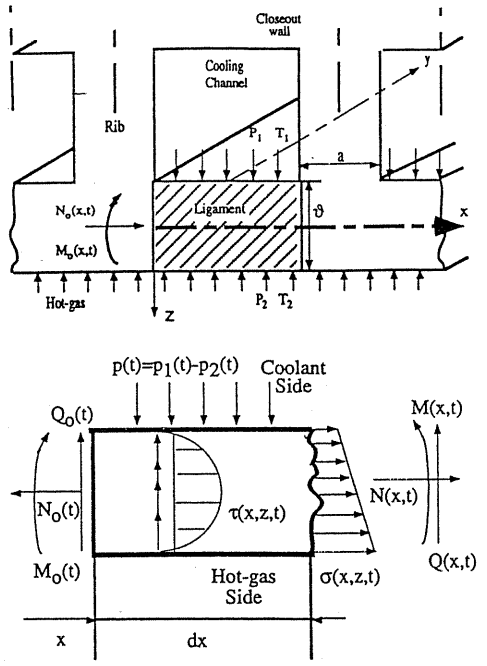

Fig. 1 Rectangular beam model of the coolant channel ligament.

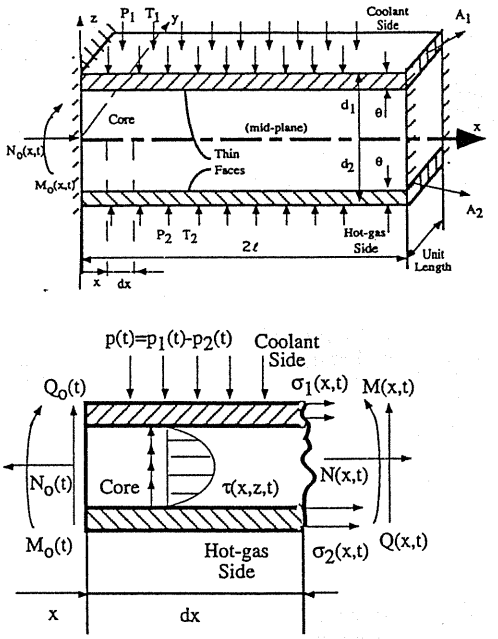

Fig. 2 Sandwich beam model of the coolant channel ligament.

stresses σ_1 and σ_2 are assumed to be constant throughout the faces, and the core is rigid in shear and bears no normal stresses.

4) The ligament temperature does not vary along the circumferential x direction because of geometrical symmetry, but there exists a thermal gradient across the wall thickness in the radial z direction.

5) The total strain ε is the sum of elastic, inelastic, and thermal strains, ε^e, ε^p, and ε^{th} on each of the cold and hot faces, i.e., $\varepsilon_i(x, t) = \varepsilon_i^e(x, t) + \varepsilon_i^p(x, t) + \varepsilon_i^{th}(x, t)$, $i = 1, 2$.

6) Uniaxial loading is applied to the sandwich beam model.

7) Due to the symmetric loading and geometric configuration, only a half-beam model is considered.

Compatibility Equations

Based on the symmetric geometry of the sandwich beam model, the expressions for the strain-displacement relation are as follows:

$$w(x, t) = w^0(x, t)$$
$$\varepsilon_i(x, t) = \frac{\partial u^0(x, t)}{\partial x} + d_i\left[\frac{\partial^2 w(x, t)}{\partial x^2}\right] \qquad i = 1, 2 \tag{2}$$

where $u^0(x, t)$ and $w^0(x, t)$ denote the displacement and deflection, respectively, at the midplane $z = 0$. The midplane strain ε^0 and midplane curvature κ are defined as

$$\varepsilon^0(x, t) = \frac{\partial u^0(x, t)}{\partial x} \qquad \kappa(x, t) = -\frac{\partial^2 w(x, t)}{\partial x^2} \tag{3}$$

Constitutive Equations

For the one-dimensional loading problem in the sandwich beam,[11] the hoop stresses in the cold and hot faces are obtained in terms of ε^0 and κ from Eqs. (2) and (3) as

$$\sigma_1 = E_1(\varepsilon^0 - d_1\kappa - \varepsilon_1^p - \varepsilon_1^{th})$$
$$\sigma_2 = E_2(\varepsilon^0 + d_2\kappa - \varepsilon_2^p - \varepsilon_2^{th}) \tag{4}$$

where the plastic strains ε_i^p, $i = 1, 2$, are obtained from the viscoplastic model.

Equilibrium Equations

Based on the free body diagram of the sandwich beam, the resultant hoop force N and bending moment M are obtained by integrating the stress over the sandwich beam cross section as

$$N(x, t) = \int_{-d_2}^{d_1} \sigma_x(x, z, t)\, dz = \sigma_1(x, t)A_1 + \sigma_2(x, t)A_2 \tag{5a}$$

$$M(x, t) = \int_{-d_2}^{d_1} \sigma_x(x, z, t)z\, dz = \sigma_2(x, t)A_2d_2 - \sigma_1(x, t)A_1d_1 \tag{5b}$$

Governing Equations

Combining Eqs. (2–5) and a rearrangement yield the following pair of coupled nonlinear partial differential equations (PDEs) with t and space x as independent variables. Details are given by Dai and Ray[11]:

$$\frac{\partial u^0(x, t)}{\partial x} = \frac{1}{A_1A_2E_1E_2(d_1 + d_2)^2}[(A_1d_1^2E_1 + A_2d_2^2E_2)N(x, t) + (A_1d_1E_1 - A_2d_2E_2)M(x, t)] + \frac{d_2}{(d_1 + d_2)}[\varepsilon_1^{th}(x, t) + \varepsilon_1^p(x, t)] + \frac{d_1}{(d_1 + d_2)}[\varepsilon_2^{th}(x, t) + \varepsilon_2^p(x, t)] \tag{6}$$

$$\frac{\partial^2 w(x, t)}{\partial x^2} = \frac{-1}{A_1A_2E_1E_2(d_1 + d_2)^2}[(A_1d_1E_1 - A_2d_2E_2)N(x, t) + (A_1E_1 + A_2E_2)M(x, t)] + \frac{1}{(d_1 + d_2)}\{d_2[\varepsilon_1^{th}(x, t) + \varepsilon_1^p(x, t)] - d_1[\varepsilon_2^{th}(x, t) + \varepsilon_2^p(x, t)]\} \tag{7}$$

where the stress resultants N and M are obtained from the equilibrium conditions as follows:

$$N(x, t) = -N_0(t) \tag{8}$$

$$M(x, t) = M_0(t) + p(t)lx - [p(t)x^2/2] \tag{9}$$

in terms of the unknown reaction bending moment M_0 and hoop force N_0 at the junction of the ligament with the rib (i.e., at $x = 0$), which are to be determined from the boundary conditions in this statically indeterminate structure. At a fixed instant of t the previous PDEs can be solved for known plant variables, namely, chamber pressure, coolant pressure, and wall temperatures on both hot and cold sides, and the inelastic strains ε_1^p and ε_2^p with x as the independent variable, along with the boundary conditions presented next.

Boundary Conditions

Five boundary conditions that are needed for solving the coupled differential Eqs. (6) and (7) with respect to x, and two unknown variables, namely, reaction moment M_0 and force N_0 at each instant of t are presented next:

$$\text{at } x = 0: \quad \frac{dw(x, t)}{dx} = 0, \quad w(x, t) = 0, \quad u^0(x, t) = -l\varepsilon_B \tag{10a}$$

$$\text{at } x = l: \quad \frac{dw(x, t)}{dx} = 0, \quad u^0(x, t) = 0 \tag{10b}$$

where

$$\varepsilon_B = \alpha_BT_B - \alpha_0T_0 \tag{10c}$$

and $x = l$ corresponds to the center section of the ligament, T_B and α_B are the closeout wall temperature and linear coefficient of thermal expansion, respectively, and T_0 is the known reference temperature of the closeout wall.

Closed-Form Solution of the Sandwich Beam Model Equations

Applying Eqs. (8) and (9) along with the boundary conditions in Eqs. (10) into the governing Eqs. (6) and (7), the time-dependent reaction force N_0 and moment M_0 are obtained as:

$$N_0(t) = \bar{C}\left[\bar{I}_1^{th}(t) - \varepsilon_B(t) + \frac{1}{l}\int_0^l \bar{I}_1^p(x, t)\, dx\right] - \frac{\bar{B}}{(d_1 + d_2)}\left[\bar{I}_2^{th}(t) + \frac{1}{l}\int_0^l \bar{I}_2^p(x, t)\, dx\right] \tag{11}$$

$$M_0(t) = -\frac{p(t)l^2}{3} + \bar{B}\left[\bar{I}_1^{th}(t) - \varepsilon_B(t) + \frac{1}{l}\int_0^l \bar{I}_1^p(x, t)\, dx\right] - \frac{\bar{A}}{(d_1 + d_2)}\left[\bar{I}_2^{th}(t) + \frac{1}{l}\int_0^l \bar{I}_2^p(x, t)\, dx\right] \tag{12}$$

where

$$\bar{A} = \frac{A_1d_1^2E_1 + A_2d_2^2E_2}{A_1A_2E_1E_2(d_1 + d_2)^2} \qquad \bar{B} = \frac{A_1d_1E_1 - A_2d_2E_2}{A_1A_2E_1E_2(d_1 + d_2)^2}$$

$$\bar{C} = \frac{A_1E_1 + A_2E_2}{A_1A_2E_1E_2(d_1 + d_2)^2} \qquad \bar{I}_1^{th} = \frac{(d_2\varepsilon_1^{th} + d_1\varepsilon_2^{th})}{(d_1 + d_2)}$$

$$\bar{I}_1^p = \frac{(d_2\varepsilon_1^p + d_1\varepsilon_2^p)}{(d_1 + d_2)} \qquad \bar{I}_1^p = \frac{(d_2\varepsilon_1^p + d_1\varepsilon_2^p)}{(d_1 + d_2)}$$

$$\bar{I}_2^{th} = (\varepsilon_2^{th} - \varepsilon_1^{th}) \qquad \bar{I}_2^p = (\varepsilon_2^p - \varepsilon_1^p)$$

Then the hoop stresses on the two thin faces of the sandwich beam, which are the inputs to the viscoplastic model,[9] can be obtained in terms of the force and moment from Eqs. (5) as

$$\sigma_1(x, t) = \frac{d_2 N(x, t) - M(x, t)}{A_1(d_1 + d_2)}$$
$$\sigma_2(x, t) = \frac{d_1 N(x, t) + M(x, t)}{A_2(d_1 + d_2)} \tag{13}$$

A closed form solution of the radial deflection $w(x, t)$ at the midplane of the ligament can be obtained by substituting the boundary conditions in Eqs. (10), and Eqs. (11–13) into the governing differential Eqs. (6) and (7) as

$$w(x, t) = \frac{\bar{C}x^2 p(t)}{6}\left(l^2 - lx + \frac{x^2}{4}\right) + \frac{1}{(d_1 + d_2)}\left(\frac{x^2}{2l}\int_0^l \bar{I}_2^p \, d\xi - \int_0^x \int_0^\eta \bar{I}_2^p \, d\xi \, d\eta\right) \tag{14}$$

The first term on the right-hand side (RHS) of Eq. (14) represents the reversible components of the radial deflection that vanish in the absence of any pressure and temperature difference across the ligament when the cycle is completed. The second term on the RHS of Eq. (14) represents the deflection resulting from inelastic strain ratcheting induced by thermomechanical loading that contributes to permanent bulging-out and progressive thinning of the coolant channel ligament. Therefore, the irreversible deflection at the midplane of the ligament, denoted as $w^I(x, t)$, in the second term of Eq. (14) is expressed as

$$w^I(x, t) = \frac{1}{(d_1 + d_2)}\left(\frac{x^2}{2l}\int_0^l \bar{I}_2^p \, d\xi - \int_0^x \int_0^\eta \bar{I}_2^p \, d\xi \, d\eta\right) \tag{15}$$

Thinning Model of the Coolant Channel Ligament

Experimental studies by Hannum et al.[12] show the evidence of incremental bulging-out and progressive thinning at the center of the ligament after each firing cycle for the OFHC copper material. Porowski et al.[7] proposed a relationship for linear variations in the thickness of the coolant channel ligament based on experimental observations of the deformed shapes. Based on the details reported by Porowski et al.,[7] the time-dependent normalized thinning with respect to the initial thickness ϑ_0 of the ligament at its center[7] is obtained as

$$\bar{\tau}(t) = \left[\left(\frac{4l}{a} + 1\right) w(t)\right] \Big/ \left[\frac{4l}{a}\left(\frac{2l}{a} + 1\right)\right] \Big/ \vartheta_0 \tag{16}$$

The instantaneous thickness of the deformed beam is updated by subtracting the time-dependent thinning from the original thickness:

$$\vartheta(t) = \vartheta_0 - \tau(t) \tag{17}$$

Following Fig. 3, the sandwich beam model is updated with the current ligament thickness $\vartheta(t)$ in Eq. (1).

Damage Analysis and Remaining Life Prediction of the Coolant Channel Ligament

We define the damage in the ligament as a continuous function of time in the deterministic setting–following the industrial practice of denoting creep damage and fatigue damage in the scale of 0 to 1. The damage $D(t)$ in the thrust chamber wall is thus expressed in terms of the current state of normalized thinning $\bar{\tau}(t)$ of the ligament and its critical value $\bar{\tau}^*$, beyond which the thinning process becomes unstable (i.e., the tensile rupture is imminent) as

$$D(t) = \bar{\tau}(t)/\bar{\tau}^* \tag{18}$$

The critical value $\bar{\tau}^*$, which is a positive fraction is experimentally determined for each material[6,7] for a given range of thermomechanical load; $\bar{\tau}^*$ increases with increased ductility of the ligament material. It should be noted, however, that the definition of damage is not unique; the damage model may depend on the specific application.

The end of useful service period t_f at which the damage $D_{cr}(t_f)$ reaches unity [i.e., $\bar{\tau}(t_f) = \bar{\tau}^*$] denotes the total life of the thrust chamber wall ligament. Clearly, t_f is dependent on the complete history of thermomechanical load to which the ligament has been subjected. If the actual thermomechanical load is different from the anticipated load, the predicted total life t_f should be recalculated based on the load history up to the current t and the updated profile of the anticipated load beyond t. In that case, the predicted instant failure, and hence, the remaining service life $\mathcal{L}$ becomes time dependent:

$$\mathcal{L}(t) = t_f(t) - t \tag{19}$$

Model Solution Approach

The PDEs (6) and (7) are approximated via spatial discretization as a set of ordinary differential equations (ODEs) where the number of nodes is selected to be 11 for half of the ligament. Figure 3 illustrates a concept for simultaneously solving the structural and creep damage model equations of the coolant channel ligament. A causal relationship exists between the PDEs with respect to the spatial variable x in the sandwich beam model and those with respect to the temporal variable t in the viscoplastic model in Fig. 3. As explained in the previous section, the tensile force, bending moment, and stresses in the coolant channel ligament are generated from the sandwich beam model for given boundary conditions, plant variables, and inelastic strain $\varepsilon_1^p(x, t)$ and $\varepsilon_2^p(x, t)$ at each instant of time. The plastic strains at each node are obtained from the viscoplastic model as shown in Fig. 3 at each instant of time in terms of the initial conditions of the plastic strains and internal state variables, and stresses at each node.

A closed-form solution of the midplane deflection of the coolant ligament is derived at each node in the spatial direction through the sandwich beam model and fed into the thinning damage model in Fig. 3. The damage variable is defined in Eq. (18) as thickness reduction of the coolant channel ligament normalized with respect to the original thickness, and this information is fed back to the sandwich beam model to update the geometric deformation at each instant of the

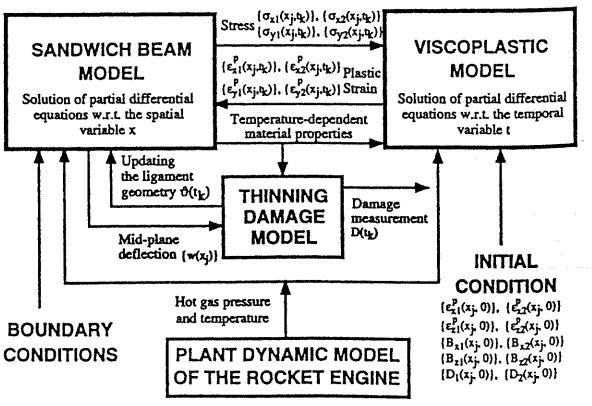

Fig. 3 Schematic diagram for solving the creep damage model.

time during the operating cycles. These calculations can be easily performed on-line for life prediction and damage mitigating control. The time-dependent coolant wall temperature and fluid pressure acting on the ligament, which are either measured or generated from the nonlinear plant dynamic model of the rocket engine, are the inputs to the sandwich beam model and the viscoplastic model. The set of ODEs in each model is solved by numerical integration. In contrast to the common practice of finite element analysis, the proposed life prediction model for the coolant channel ligament is computationally much more efficient with comparable accuracy on damage prediction. Details of the model verification are given next.

Model Verification

The structural model of the coolant channel ligament is verified through comparison with a finite element model of the thrust chamber coolant wall for two different materials, namely, OFHC copper and NARloy–Z. In the proposed model, structural geometry of the ligament and displacement of the closeout wall are used to obtain the required boundary conditions. The geometrical dimensions of the thrust chamber of a typical rocket engine with 72, 390, and 540 coolant channels are listed as sets 1, 2, and 3 in Table 1. Figure 4 shows the time histories of the process variables, namely, cold-side ligament temperature T_1, the hot-side ligament temperature T_2, closeout wall temperature T_B, and the pressure load p acting on the ligament for typical operating cycles of duration 3.5 and 408 s. Each of these cycles includes startup and heating, referred to as the hot phase of a cycle, and shutdown and cooling, referred to as the cold phase of a cycle. For OFHC copper, the cycle of 3.5 s represents the test condition of the plug nozzle module tested by Armstrong.[4,5] For NARloy–Z, the startup and heating cycle of 408 s, is the typical operating

Table 1 Geometrical dimensions of the coolant channel ligament of the cylindrical thrust chamber

Channel dimension, in./mm	Set 1 with 72 channels	Set 2 with 390 channels	Set 3 with 540 channels
Ligament length $2l$	0.0664/1.686	0.04/1.016	0.029/0.7338
Ligament thickness ϑ_0	0.035/0.889	0.028/0.711	0.028/0.711
Rib length a	0.05/1.27	0.045/1.143	0.0325/0.8255

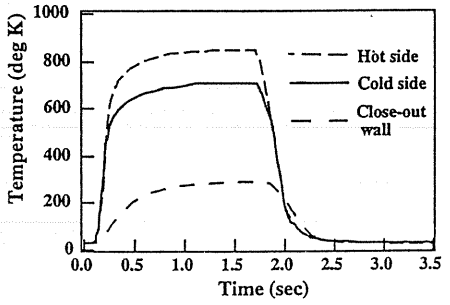

Cyclic Temperature Profile for OFHC Copper

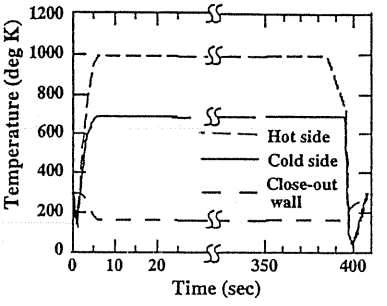

Cyclic Temperature Profile for NARloy-Z

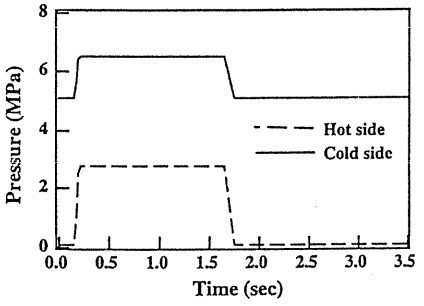

Cyclic Pressure Profile for OFHC Copper

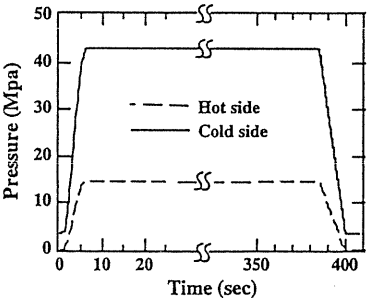

Cyclic Pressure Profile for NARloy-Z

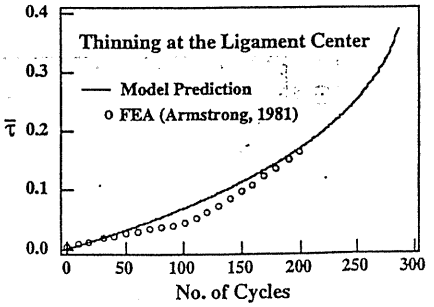

Thinning Profile for OFHC copper

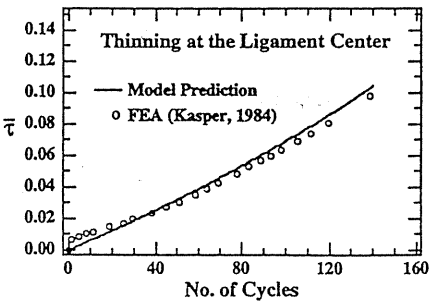

Thinning Profile for NARloy-Z

Fig. 4 Comparison of the life prediction model with finite element analyses.

time of a spacecraft rocket engine.[6] The results of model prediction are then compared with those of the finite element analyses conducted on the plug nozzle thrust chamber for OFHC copper using the data of set 1 in Table 1 and on a rocket engine thrust chamber for NARloy–Z using the data of sets 2 and 3.

As the temperature is rapidly increased during the heating part of an operating cycle, the hoop stress changes from tension to large compression due to the restricted expansion of the hot ligament imposed by the relatively cool closeout wall. Thus, during the heating process, large plastic compressive strains are induced in the ligament. The stress overshoot occurs at the instant of maximum temperature difference between the ligament and closeout wall during the cycle. In the hot phase of the cycle, the magnitude of the compressive stress relaxes to a lower steady state after reaching the peak. If the ligament is exposed to a higher temperature environment and a longer time period, the stress relaxation phenomenon would become more prominent. The rapid increase in ligament thinning occurs during the heat-up and chill-down transients that are of similar characteristics for both OFHC copper and NARloy–Z. During a thermomechanical loading transient, the back stress lags behind the actual stress. This results in a large rate of change in the inelastic strains, which eventually causes a rapid increment of the ligament thinning. The inelastic strains during the temperature and pressure transients change more rapidly than those in the steady-state conditions when the thermomechanical loading is nearly constant. The critical values of $\bar{\tau}^*$, beyond which the thinning process tend to become unstable, are reported to be ~0.37 for OFHC copper[7] and ~0.08 for NARloy–Z.[6] The lower $\bar{\tau}^*$ for NARloy–Z is attributed to its less ductility relative to OFHC copper. It follows from Fig. 4 that, under the respective thermomechanical loading condition, the expected safe life of the OFHC copper ligament is ~250 cycles and that for NARloy–Z is ~125 cycles. It should be noted, however, that the pressure loading for NARloy–Z is selected to be about 135% of the design specifications for compatibility with the results of finite element analysis reported by Kasper.[6] At nominal (100%) pressure loading, the proposed model predicts the expected safe life of NARloy–Z to be ~500 cycles.[6]

Figure 4 compares the results of progressive thinning predicted by the present life prediction model with the finite element analysis data reported by Armstrong[4,5] and Kasper[6] for OFHC copper and NARloy–Z, respectively. The close agreement between model prediction and finite element analyses indicates that the model, presented in this article, accurately predicts the midplane deflection of the ligament and captures the mechanics of creep rupture of the thrust chamber wall. Therefore, this model is capable of calculating the current damage $D(t)$ in Eq. (18) and predicted the remaining service life $\mathcal{L}(t)$ in Eq. (19). One of the important features of this life prediction model is its numerical efficiency. For example, one typical firing cycle takes about 0.35 h on an IBM mainframe computer for the finite element model given by Armstrong,[5] whereas it takes only about 0.5 s on an Indy Silicon Graphics workstation, and less than 2 s on a Pentium for the proposed model.

Parametric Studies

The life-prediction model presented in this article is capable of providing general information for better understanding of the failure mechanism and nonlinear behavior of a rocket engine thrust chamber wall, and allows design optimization with low computational cost. Specifically, this model can be used to investigate the impact of several factors, such as materials selection and mechanical design, thermomechanical loading conditions and their duration, on structural durability of the thrust chamber. To this effect, the following criteria for the thrust chamber design are discussed: 1) different materials, namely, OFHC copper and NARloy–Z; 2) different ligament dimensions, namely, the number of coolant channels being 390 and 540; 3) different mechanical loading acting on the ligament; 4) different thermal loading acting on the ligament; and 5) different operational cycle duration, namely, a short cycle of 3.5 s and an extended cycle of 485 s. Simulation experiments were conducted to investigate the previous five cases one at a time. In each case, unless specified otherwise, the time history of the thermomechanical process variables, namely, ligament temperatures at T_1 and T_2, the T_B, and the pressure acting on the ligament are as shown in the top two plots on the left side of Fig. 4 for a cycle duration of 3.5 s, and on the top two plots on the right side for a cycle duration of 408 s.

Effect of Material Behavior (OFHC Copper and NARloy–Z)

This section presents the results of analyses for two different ligament materials, namely, OFHC copper and NARloy–Z, under identical channel dimension, thermomechanical loading, and operational cycle duration. The geometric dimensions of the coolant channel ligament correspond to set 1 with 72 channels as listed in Table 1. Profiles of $\bar{\tau}$ at the ligament center are plotted in Fig. 5a for OFHC copper and NARloy–Z materials during the first three cycles. Even though two materials are subjected to identical thermomechanical cycling, their stress/strain responses are quite different resulting from dissimilar thermal ratcheting phenomena caused by incomplete strain reversal. The cyclic mean stress of NARloy–Z is close to zero since the tensile and compressive loads are almost symmetric. In contrast, the mean stress for OFHC copper is tensile due to non-symmetric tensile and compressive loading as seen in Fig. 5a. NARloy–Z appears to have a higher stress relaxation rate than OFHC copper during both tensile and compressive holding periods. The stresses for OFHC copper exhibit a few cycles of transitions due to the initial stress hardening, whereas the stresses for NARloy–Z are almost perfectly periodic during the entire cyclic loading. Since OFHC copper is more ductile than NARloy–Z, the initial compressive plastic strain of OFHC copper is more pronounced than that of NARloy–Z.

Once substantial bulging occurs, the thermal and structural characteristics in the vicinity of the bulging region change because of the deformation in geometry. Since this deformation is updated at each instant of time in the life prediction model in Fig. 3, the resulting effects on creep ratcheting are

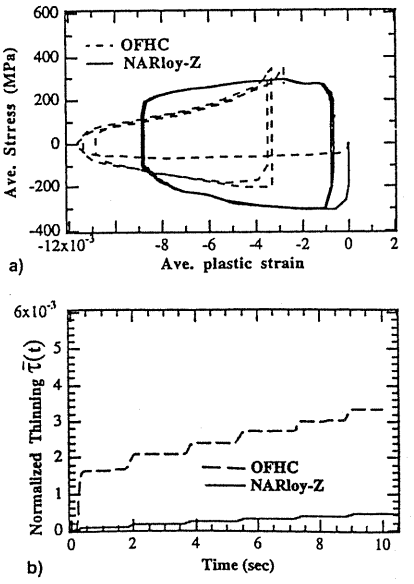

Fig. 5 a) Cyclic stress/strain hysteresis loop and b) normalized thinning $\bar{\tau}(t)$ during the first three cycles.

more severe for OFHC copper than those for NARloy–Z. Consequently, OFHC copper suffers from a larger bulging-out as shown in Fig. 5b. The plastic flow and bulging-out of the inner wall for NARloy–Z are smaller than those for OFHC copper. This prediction is consistent with the damage observed in actual test chambers as reported by Hannum et al.[12] Thinning of an OFHC copper ligament is approximately 10 times larger than that of a NARloy–Z ligament as seen in Fig. 5b. Both simulation results and experimental observations demonstrate that NARloy–Z, under the identical thermomechanical loading, yields a longer service life of coolant channels than OFHC copper.

Effect of Ligament Dimensions (Number of 390 and 540 Channels)

This section presents the results of analyses for different number of coolant channels under identical thermomechanical cyclic loading and duration for each of the two materials, OFHC copper and NARloy–Z. Dimensions for different configurations of the coolant channel ligaments correspond to sets 2 and 3 with 390 and 540 channels, in Table 1. Figures 6a and 6b show $\bar{\tau}$ of the ligament for OFHC copper and NARloy–Z, respectively, for the two different ligament configurations. For both configurations, $\bar{\tau}$ for OFHC is approximately 10 times larger than that for NARloy–Z, due to the different material characteristics as discussed earlier. If the ratio of the length-to-thickness is made smaller for 540 channels, the ligament becomes less flexible resulting in decreased bulging-out and, therefore, longer service life is attained.

Effect of Mechanical Loading

To assess the role that pressure loading plays on the so-called doghouse effect[12] in the thrust chamber coolant wall, the coolant ligament has been analyzed for different pressure (i.e., mechanical) loading under identical ligament configuration, temperature (i.e., thermal) loading, and operational cycle duration. The time history of the mechanical loading, namely, the magnitude of pressure difference acting on the ligament, $\Delta P(t) = [P_1(t) - P_2(t)]$, is increased twofold. The temperature loading history is maintained at the same level as that on the top left corner of Fig. 4, and the dimensions of the coolant channel ligament correspond to 72 channels in set 1 of Table 1.

Creep ratcheting that is largely induced by the pressure difference is discussed by Porowski et al.[7] Bending stresses due to the cyclic pressure loading cause a plastic deformation and bulging-out of the ligament during each cycle. As the pressure difference is increased twofold, plastic strain and creep ratcheting rate per cycle for OFHC copper change much more significantly than those for NARloy–Z, which is less ductile. Normalized thinning of the ligament for a twofold increase in pressure loading is shown in Figs. 7a and 7b for OFHC copper and NARloy–Z, respectively. The thinning rate is increased about two times for both OFHC copper and NARloy–Z.

Effect of Thermal Loading

Hannum et al.[12] and Quentmeyer[10] reported that the cycles to failure could be correlated with either the hot-side ligament temperature or the temperature difference between the hot-side of the ligament and closeout wall. In order to determine the effects of thermal loading on the thrust chamber life, four sets of different temperatures are investigated under identical pressure loading, ligament dimension, and operational cycle. The time history of the pressure (mechanical) loading is maintained at the same level as that on the left side of Fig. 4 and the dimensions of the coolant channel ligament correspond to 72 channels in set 1 of Table 1. For each of the following four cases T_B was kept unchanged.

1) Case A serving as the baseline case where the superscript * indicates the reference profile for T_1 and T_2 as shown on the top left corner of Fig. 4.

2) Case B where T_2 is increased by about 150 K over T_2^* during the hot phase and T_1 is kept equal to T_1^*.

3) Case C where T_1 is increased to T_2^* during the hot phase and T_2 is kept equal to T_2^*. Therefore, there is no temperature difference across the ligament.

4) Case D where T_1 is decreased by about 150 K from T_1^* during the hot phase and T_2 is kept equal to T_2^*.

The plastic strain range in the ligament is largely dependent on the thermal strain range, which is a function of the transient difference between the average ligament temperature and the closeout wall temperature. Therefore, case B and case C yield a higher effective plastic strain range than case A due to increased average temperature of the ligament. In contrast, case D yields smaller effective plastic strain range and compressive mean plastic strain than case A due to decreased average temperature of the ligament. The rationale is that the average ligament temperature in case D is decreased during

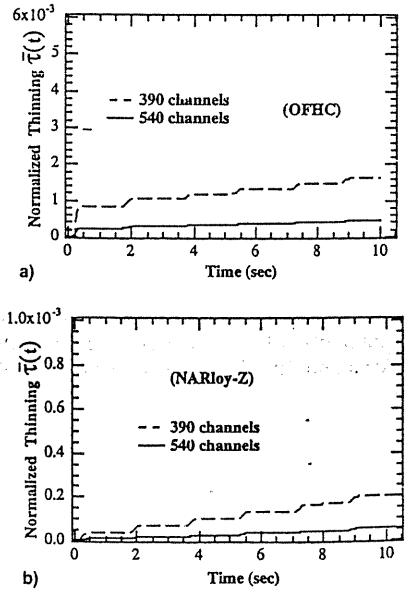

Fig. 6 a) Normalized thinning $\bar{\tau}(t)$ (OFHC) and b) (NARloy–Z) for different dimensions.

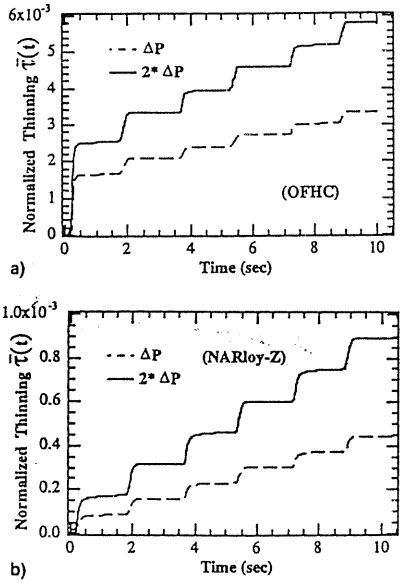

Fig. 7 a) Normalized thinning $\bar{\tau}(t)$ (OFHC) and b) (NARloy–Z) for different pressure loading.

the hot phase, the magnitudes of both tensile and compressive stresses are reduced, and the initial plastic strain is less compressive.

Figures 8a and 8b plot the stress/strain hysteresis loops for OFHC copper and NARloy–Z under the previous four different cases. Although the average ligament temperature is increased for both case B and case C, there is no temperature difference across the ligament in case C, whereas this difference does exist in case B. The magnitude of the compressive mean plastic strain in case C is larger than that in case B as seen in Figs. 8a and 8b because the ligament is subjected to thermally induced bending in case B due to the constraints at the two ends imposed by the relatively cool closeout wall. This thermally induced bending partially compensates the bulging-out effect resulting from the pressure loading[13]; there is, however, no such effect in case C. Therefore, the resultant bulging-out due to both pressure and thermally induced bending in case B are less pronounced than that in case C as seen in Figs. 9a and 9b for both OFHC copper and NARloy–Z, respectively. Case D has the longest service life for both materials since the average ligament temperature is the lowest among all four cases. This observation reveals that the service life of the coolant wall can be improved not only by lowering the average ligament temperature, but also by increasing the temperature difference across the ligament. The latter phenomenon is more significant in OFHC copper than in NARloy–Z because the benefits of thermally induced bending are more effective due to larger ductility of OFHC copper.

Effect of Loading Cycle Duration

The effects of different loading cycle duration on the service life of the coolant channel wall of the thrust chamber was investigated for two types of thermomechanical loading cycle duration by Arya and Arnold.[13] Figure 10a depicts $\bar{\tau}$ of the OFHC copper ligament as a function of the number of cycles for both the short and extended loading cycles. A comparison of the $\bar{\tau}$ curves for these two loading cycles reveals that thinning is larger for the extended cycle. This happens because

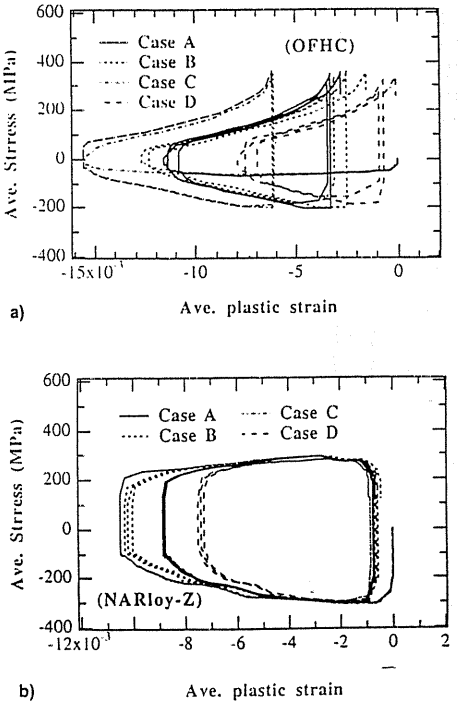

Fig. 8 Cyclic stress/strain hysteresis loop for a) OFHC and b) NARloy–Z for different temperature loading.

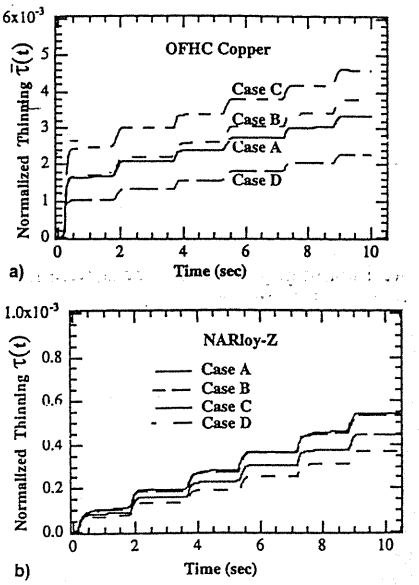

Fig. 9 Normalized thinning $\bar{\tau}(t)$ for a) OFHC and b) NARloy–Z for different pressure loading.

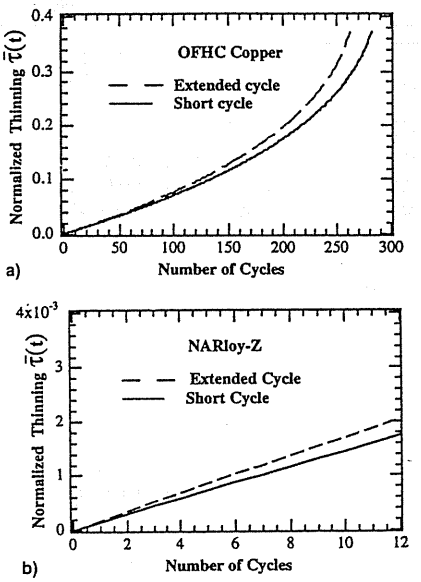

Fig. 10 Normalized thinning $\bar{\tau}(t)$ for a) OFHC and b) NARloy–Z for multiple cycles.

the plastic strain obtained from the viscoplastic model increases as the hold time is increased for the extended cycle. Therefore, the irreversible or permanent deformation of the coolant channel ligament is larger for the extended cycle than that for the short cycle. Figure 10b shows similar behavior for NARloy–Z ligaments, which is in agreement with the results reported by Arya and Arnold.[13] In summary, the bulging-out and thinning phenomena of the coolant channel ligament become more pronounced for both OFHC copper and NARloy–Z as the duration of the loading cycle is increased.

Summary and Conclusions

This article presents a continuous-time damage and life prediction model of the coolant channel ligament in the thrust chamber of reusable rocket engines under both steady-state and transient operations. The structural part of this model is built upon the theories of sandwich beam and viscoplasticity.

The modeling approach consists of analyzing the incremental bulging-out and progressive thinning of the ligament in each firing cycle by taking the effects of geometric deformation into consideration. The model has been validated by comparison with finite element models for two different materials, namely, (OFHC) and NARloy–Z. The close agreement with the finite element model indicates that the proposed life prediction model can capture the failure mechanics (i.e., creep rupture) of the thrust chamber wall by calculating the midplane deflection of the ligament. The life prediction model is numerically much more efficient than the finite element model with comparable accuracy; however, relative to the finite element model, the overall scope of this model is limited. For example, one typical firing cycle takes about 0.35 h on an IBM mainframe computer for the finite element model given by Armstrong,[5] whereas it takes about 0.5 s on an Indy Silicon Graphics workstation, and less than 2 s on a Pentium for the proposed model. The proposed model is suitable for on-line life prediction and for the damage mitigating control of reusable rocket engines for which the finite element model is not adequate.

The predicted life of the coolant channel wall is influenced by several factors including the ligament material, configuration and design of the channel, chamber pressure, wall temperature, and loading cycle duration. These effects have been investigated via parametric studies, and the following conclusions are derived:

1) The proposed model provides simplified analyses that can predict the failure behavior of the coolant channel wall of rocket engines. The failure phenomena, regardless of whether the material is OFHC copper or NARloy–Z, are characterized by thinning at the ligament center. The deformation of an OFHC copper ligament, under identical thermomechanical loading, is predicted to be larger than for that of a NARloy–Z ligament, which is less ductile.

2) Increasing the number of coolant channels such that the ratio of the ligament length-to-thickness is reduced is one of the feasible approaches to life extension of the thrust chamber.

3) The pressure difference across the coolant channel ligament is a cause of the bulging-out phenomenon and the ligament thinning increases with the pressure difference.

4) Decreasing the coolant wall temperature is a possible solution to reduce the thinning of the thrust chamber wall. The thermally induced bending, resulting from a temperature difference across the ligament, tends to retard the bulging-out process due to the pressure loading, and therefore, improves the service life of the thrust chamber, especially for the OFHC copper material.

5) The magnitude of the bulging-out and thinning of the coolant channel ligament for both OFHC copper and NARloy–Z materials is dependent on the duration of the loading cycle. The bulging-out process is more pronounced for the extended cycle than that for the short loading cycle.

Acknowledgments

The work reported in this article was supported in part by NASA Lewis Research Center under Grants NAG 3-1240 and NAG3-1673, the National Science Foundation under Research Grants ECS-9216386 and DMI-9424587, and the Electric Power Research Institute under Contract EPRI RP8030-5. The authors acknowledge the benefits of discussions with Marc Carpino of Penn State University and Carl F. Lorenzo of NASA Lewis Research Center.

References

[1]Ray, A., Wu, M.-K., Carpino, M., and Lorenzo, C. F., "Damage-Mitigating Control of Mechanical Systems: Part I—Conceptual Development and Model Formulation," *Journal of Dynamic Systems, Measurement, and Control*, Vol. 116, No. 3, 1994, pp. 437–447.

[2]Ray, A., Wu, M.-K., Carpino, M., and Lorenzo, C. F., "Damage-Mitigating Control of Mechanical Systems: Part II—Formulation of an Optimal Policy and Simulation," *Journal of Dynamic Systems, Measurement, and Control*, Vol. 116, No. 3, 1994, pp. 448–455.

[3]Ray, A., Dai, X., Wu, M.-K., Carpino, M., and Lorenzo, C. F., "Damage-Mitigating Control of a Reusable Rocket Engine," *Journal of Propulsion and Power*, Vol. 10, No. 2, pp. 225–234.

[4]Armstrong, W. H., "Structural Analysis of Cylindrical Thrust Chamber," Vol. I, Final Rept., NASA Lewis Research Center, NASA CR-159552, Contract NASA-21361, March 1979.

[5]Armstrong, W. H., "Structural Analysis of Cylindrical Thrust Chamber," Vol. II, Final Rept., NASA Lewis Research Center, NASA CR-165241, Contract NASA-21953, March 1981.

[6]Kasper, H. J., "Thrust Chamber Life Prediction," *Advanced High Pressure O2/H2 Technology*, NASA Marshall Flight Center, NASA CP 2372, Huntsville, AL, 1984, pp. 36–43.

[7]Porowski, J. S., O'Donnell, W. J., Badlani, M. L., and Kasraie, B., "Simplified Design and Life Prediction of Rocket Thrust Chambers," *Journal of Spacecraft and Rockets*, Vol. 22, No. 2, 1985, pp. 181–187.

[8]Robinson, D. N., and Arnold, S. M., "Effects of State Recovery on Creep Buckling Under Variable Loading," *Journal of Applied Mechanics*, Vol. 57, June 1990, pp. 313–320.

[9]Freed, A. D., "Structure of a Viscoplastic Theory," Constitutive Equations and Life Prediction Models for High Temperature Applications Symposium, NASA Lewis Research Center, NASA TM-100749, sponsored by American Society of Mechanical Engineers, Berkeley, CA, June 1988.

[10]Quentmeyer, R. J., "Experimental Fatigue Life Investigation of Cylindrical Thrust Chambers," NASA Lewis Research Center, NASA TM X-73665, Cleveland, OH, July 1977.

[11]Dai, X., and Ray, A., "Damage-Mitigating Control of a Reusable Rocket Engine, Part I: Life Prediction of the Combustion Coolant Wall," *ASME Winter Annual Meeting*, DSC-Vol. 55-2, Chicago, IL, Nov. 1994, pp. 1067–1073; also *Journal of Dynamic Systems, Measurement, and Control* (to be published).

[12]Hannum, N. P., Kasper, H. J., and Pavli, A. J., "Experimental and Theoretical Investigation of Fatigue Life in Reusable Rocket Thrust Chambers," NASA Lewis Research Center, NASA TM X-73413, July 1976.

[13]Arya, V. K., and Arnold, S. M., "Viscoplastic Analysis of an Experimental Cylindrical Thrust Chamber Liner," *AIAA Journal*, 1992, Vol. 30, No. 3, 1992, pp. 781–789.